# Two-stage chance-constrained programming for system optimization under uncertainty

Yu Yang

2024 IEEE International Systems Conference (SysCon) | 979-8-3503-5880-3/24/$31.00 ©2024 IEEE | DOI: 10.1109/SysCon61195.2024.10553519

*Abstract*— **This study focuses on the two-stage stochastic program (SP) with chance constraints for decision-making in system optimization under normally-distributed uncertainties. At stage-I, the integer decision variables are determined such that the expected objective function is optimized and operational constraints can be satisfied with high chance. Once the uncertainty is realized, the optimal stage-II decision is made accordingly to adjust recourse operations. The introduction of chance constraints in comparison with traditional SP helps mitigation of system conservativeness because the worst-scenario less likely occurs and override operations can be employed to prevent catastrophic outcomes. The resulting chance-constrained two-stage SP (CC-SP) is solved through the linear decision-rule in which stage-II variables are parameterized by uncertainties. Such an optimization problem can be reformulated as a mixed-integer second-order cone program that is solved efficiently. Furthermore, the posterior evaluation together with the Balas cut is integrated with the CC-SP to improve the solution quality. A refinery optimization problem is solved through the proposed scheme to verify the computational efficiency and probabilistic feasibility.**

## I. Introduction

The implementation of model-based sequential system optimization plays a vital role in enhancing the profitability, safety, and sustainability of chemical, power, and water plants. However, because of the uncertainties arising from the raw material supply, operating conditions fluctuation, or the incomplete system knowledge, deterministic optimal solutions may not achieve the desired performance or even become infeasible in practice. Consequently, the optimization under uncertainties has emerged as an essential research area for decades [1], [2], [3], [4], [5], [6]. Several comprehensive reviews have been published by Sahinidis [7] and Grossmann [8] to discuss methodologies and applications related to this field.

This work aims to address uncertainties in the optimal decision making through the chance-constrained two-stage stochastic programming (CC-SP). The entire decision process is divided into two stages. At stage-I, before uncertainties are realized, the optimization focuses on maximizing expected profit by taking all possible scenarios into account and allowing for a few infeasible cases. At stage-II, once uncertainties are realized, the recourse operations are undertaken accordingly. This formula is particularly suitable when sufficient information is available to characterize the probabilistic properties of uncertain parameters and override operations can be made to mitigate undesired outcomes. The two-stage SP is traditionally solved by the sampling-based method. Namely, multiple samples are drawn from the distribution of uncertain parameters to generate a number of scenarios. Then, the original SP is approximated by a large-scale deterministic optimization over all generated scenarios. This scenario-based approximation leads to high computational demand and usually requires using the Benders [9], [10] or Lagrangians [11], [12], [13] decomposition to reduce the computational complexity.

The integration of chance constraints into two-stage SP further increases computational complexities. Luedtke [15] proposed a branch-and-cut method to solve CC-SP. Liu et al. [14] discussed the two-stage decision process with normal and recovery operations. The probabilistic constraints were incorporated into this scheme to avoid abusing recovery operations. Their algorithms introduced a binary variable and an additional optimization problem for each scenario to create tighter cutting planes. Even though it reduced the solving time, how to handle the unseen scenarios was not addressed in that paper. The author has proposed an improved strategy to generate cutting planes without the need of solving additional optimization problems, and thereby saving more computational time [16].

In summary, conventional scenario-based methods for CC-SP suffer from two issues. Firstly, the introduction of binary variables for each sampled scenario significantly escalates computational demands, rendering the algorithm non-scalable. Secondly, the probabilistic feasibility of the solution under unseen scenarios cannot be guaranteed. Compared with the existing scenario-based methods, two innovations are presented in this paper to solve CC-SP:

(1) We utilize a linear decision-rule [17] to parameterize stage-II variables, allowing the conversion of CC-SP into a mixed-integer nonlinear program (MINLP) that can be solved to the global optimum within a certain relative gap. More importantly, the linear decision-rule is sampling-free, making its solution universally applicable across any possibilities. In fact, the capability of linear decision-rule in stochastic programming has been proved in recent literature [18].

(2) The baseline solution from the linear decision-rule can be improved through the scenario-based posterior evaluation and the Balas cut [19]. After solving the MINLP, stage-I variables are fixed whereas stage-II variables are re-solved for each scenario separately to quantify the solution quality more accurately. Then, the Balas cut eliminates previously visited stage-I integer solutions to enable further explorations of the solution space.

This work was supported by the National Science Foundation (NSF) with award number 2151497.

Yu Yang (yu.yang@csulb.edu) is with the Chemical Engineering Department of California State University, Long Beach, CA 90840, USA.

This paper is organized as follows. The problem formulation is presented in Section 2. The proposed solving methods including the linear decision-rule, posterior evaluation, and Balas cut are introduced in Section 3. A refinery optimization problem with operational uncertainties is solved to demonstrate the effectiveness of proposed algorithms in Section 4. In the final Section, the conclusion is drawn.

**Notation.** Throughout this paper, vectors and matrices are denoted by boldface letters. Underline and overline of variables denote their lower and upper bounds, respectively.

## II. Problem Formulation

The formulation of CC-SP is shown in (P). Both stage-I variables $\boldsymbol{x}$ and stage-II variables $\boldsymbol{y}$ are optimized to minimize the expected cost or maximize the expected profit.

$$\begin{aligned} \min_{\boldsymbol{x}} \ & \boldsymbol{q}^{\mathrm{T}}\boldsymbol{x} + \mathbb{E}_{\boldsymbol{\theta}}(Q(\boldsymbol{x},\boldsymbol{\theta})) \\ \text{s.t. } & \boldsymbol{x} \in \{0,1\} \cap \Pi, \end{aligned} \tag{P}$$

where

$$\begin{aligned} Q(\boldsymbol{x},\boldsymbol{\theta}) = \min_{\boldsymbol{y}_1,\boldsymbol{y}_2} \ & \boldsymbol{p}_1^{\mathrm{T}}\boldsymbol{y}_1 + \boldsymbol{p}_2^{\mathrm{T}}\boldsymbol{y}_2 \\ \text{s.t. } & \mathbb{P}\Big\{\boldsymbol{a}_i^{\mathrm{T}}\boldsymbol{x} + \sum_{k=1}^{K}\boldsymbol{b}_{k,i}^{\mathrm{T}}\theta_k\boldsymbol{y}_1 + \boldsymbol{c}_i^{\mathrm{T}}\boldsymbol{y}_2 \leqslant \boldsymbol{g}_i, \\ & \forall i = 1,2,\ldots,M\Big\} \geqslant 1-\epsilon, \\ & \boldsymbol{A}'\boldsymbol{x} + \sum_{k=1}^{K}\boldsymbol{B}_k'\theta_k\boldsymbol{y}_1 + \boldsymbol{C}'\boldsymbol{y}_2 = 0 \\ & \boldsymbol{0} \leqslant \boldsymbol{y}_1, \boldsymbol{0} \leqslant \boldsymbol{y}_2, \end{aligned}$$

where $\boldsymbol{p}_1$, $\boldsymbol{p}_2$, $\boldsymbol{q}$, $\boldsymbol{a}_i$, $\boldsymbol{A}'$, $\boldsymbol{b}_{k,i}$, $\boldsymbol{B}_k'$, $\boldsymbol{c}_i$, $\boldsymbol{C}'$ and $\boldsymbol{g}_i$ are known vectors and matrices, respectively. In this formulation, $\boldsymbol{\theta} \sim \mathcal{N}(\boldsymbol{\mu},\boldsymbol{\sigma}^2)$ represents independent normally-distributed uncertainties, $\Pi$ is a deterministic constraint set of $\boldsymbol{x}$, and $\epsilon$ is the user specified risk level.

Note that $M$ joint chance constraints are introduced into the stage-II formula $Q(\boldsymbol{x},\boldsymbol{\theta})$, which enables us to handle incomplete recourse problem. These chance constraints can represent the operational condition or product quality specification. In addition, the equality constraint is also considered in the stage-II formula, which usually represents the mass balance. Stage-II variables $\boldsymbol{y}$ is divided into two sub-vectors: $\boldsymbol{y}_1 \in \Re^{N_1}$ and $\boldsymbol{y}_2 \in \Re^{N_2}$. The coefficients of $\boldsymbol{y}_1$ incorporate uncertain parameters $\theta_k$ whereas $\boldsymbol{y}_2$ coefficients are all constant.

## III. Solving Method

### A. Reformulation

The linear decision-rule is developed to solve (P). Let $\boldsymbol{y}_2$ to be the function of uncertainties:

$$\boldsymbol{y}_2 = \boldsymbol{H}\boldsymbol{\theta} + \boldsymbol{w}, \tag{1}$$

where $\boldsymbol{H} = [\boldsymbol{h}_1^{\mathrm{T}};\boldsymbol{h}_2^{\mathrm{T}};\ldots;\boldsymbol{h}_{N_2}^{\mathrm{T}}] \in \Re^{N_2\times K}$ and $\boldsymbol{w} \in \Re^{N_2}$ are coefficients to be determined. Note that $\boldsymbol{y}_1$ is not parameterized because its coefficient already has uncertain parameters. Otherwise, it will lead to the quadratic terms on uncertain parameters, which cannot be solved in this paper. Substituting (1) into (P) leads to the following formula:

$$\begin{aligned} \min_{\boldsymbol{x},\boldsymbol{y}_1,\boldsymbol{H},\boldsymbol{w}} \ & \boldsymbol{q}^{\mathrm{T}}\boldsymbol{x} + \mathbb{E}_{\boldsymbol{\theta}}(\boldsymbol{p}_1^{\mathrm{T}}\boldsymbol{y}_1 + \boldsymbol{p}_2^{\mathrm{T}}(\boldsymbol{H}\boldsymbol{\theta}+\boldsymbol{w})) && \text{(CC-SP1)} \\ \text{s.t. } & \mathbb{P}\big\{\boldsymbol{a}_i^{\mathrm{T}}\boldsymbol{x} + (\boldsymbol{y}_1^{\mathrm{T}}\boldsymbol{B}_i^{\mathrm{T}} + \boldsymbol{c}_i^{\mathrm{T}}\boldsymbol{H})\boldsymbol{\theta} + \boldsymbol{c}_i^{\mathrm{T}}\boldsymbol{w} \leqslant \boldsymbol{g}_i, \\ & \forall i = 1,2,\ldots,M\big\} \geqslant 1-\epsilon, && (2) \\ & \boldsymbol{A}'\boldsymbol{x} + \sum_{k=1}^{K}\boldsymbol{B}_k'\theta_k\boldsymbol{y}_1 + \boldsymbol{C}'(\boldsymbol{H}\boldsymbol{\theta}+\boldsymbol{w}) = \boldsymbol{0}, \\ & 0 \leqslant \boldsymbol{h}_j^{\mathrm{T}}\boldsymbol{\theta} + w_j, \forall j = 1,2,\ldots,N_2, && (3) \\ & \boldsymbol{x} \in \{0,1\} \cap \Pi, \ \boldsymbol{0} \leqslant \boldsymbol{y}_1, \end{aligned}$$

where $\boldsymbol{B}_i^{\mathrm{T}} = [\boldsymbol{b}_{1,i}, \boldsymbol{b}_{2,i}, \ldots, \boldsymbol{b}_{N,i}]$. Because $\boldsymbol{y}_2$ is a linear function of uncertainty $\boldsymbol{\theta}$, Eq. (3) represents stochastic constraints to enforce the lower limit of variables $\boldsymbol{y}_2$. Based on Boole's inequality, joint chance constraints in (2) can be conservatively approximated by decomposing them into individuals:

$$\begin{aligned} \min_{\boldsymbol{x},\boldsymbol{y}_1,\boldsymbol{H},\boldsymbol{w},\boldsymbol{\gamma},\boldsymbol{\lambda}} \ & \boldsymbol{q}^{\mathrm{T}}\boldsymbol{x} + \boldsymbol{p}_1^{\mathrm{T}}\boldsymbol{y}_1 + \boldsymbol{p}_2^{\mathrm{T}}(\boldsymbol{H}\boldsymbol{\mu}+\boldsymbol{w}) && \text{(CC-SP2)} \\ \text{s.t. } & \mathbb{P}\big\{\boldsymbol{a}_i^{\mathrm{T}}\boldsymbol{x} + (\boldsymbol{y}_1^{\mathrm{T}}\boldsymbol{B}_i^{\mathrm{T}} + \boldsymbol{c}_i^{\mathrm{T}}\boldsymbol{H})\boldsymbol{\theta} + \boldsymbol{c}_i^{\mathrm{T}}\boldsymbol{w} \leqslant g_i\big\} \\ & \geqslant 1-\gamma_i, \ \forall i = 1,2,\ldots,M, \\ & \boldsymbol{A}'\boldsymbol{x} + \sum_{k=1}^{K}\boldsymbol{B}_k'\theta_k\boldsymbol{y}_1 + \boldsymbol{C}'(\boldsymbol{H}\boldsymbol{\theta}+\boldsymbol{w}) = \boldsymbol{0}, && (4) \\ & \mathbb{P}\big\{0 \leqslant \boldsymbol{h}_j^{\mathrm{T}}\boldsymbol{\theta} + w_j\big\} \geqslant 1-\lambda_j, \forall j = 1,2,\ldots,N_2, \\ & \sum_{j=1}^{N_2}\lambda_j + \sum_{i=1}^{M}\gamma_i = \epsilon, && (5) \\ & \boldsymbol{x} \in \{0,1\} \cap \Pi, \ \boldsymbol{0} \leqslant \boldsymbol{y}_1, \end{aligned}$$

where $\boldsymbol{\gamma}$ and $\boldsymbol{\lambda}$ are introduced decision variables to determine the risk level of each constraints in (2) and (3). The lower limit of $\boldsymbol{y}_2$ are also converted to individual chance constraints. Eq. (5) requires that the summation of all individual risks to be $\epsilon$. Here (CC-SP2) is a conservative approximation of (CC-SP1).

The problem (CC-SP2) still cannot be solved by the deterministic solver directly due to its stochastic nature. With normally-distributed uncertainties, (CC-SP2) can be equivalently converted into an MINLP [20]:

$$\begin{aligned} \min_{\boldsymbol{x},\boldsymbol{y}_1,\boldsymbol{H},\boldsymbol{w},\boldsymbol{\gamma},\boldsymbol{\lambda}} \ & \boldsymbol{q}^{\mathrm{T}}\boldsymbol{x} + \boldsymbol{p}_1^{\mathrm{T}}\boldsymbol{y}_1 + \boldsymbol{p}_2^{\mathrm{T}}(\boldsymbol{H}\boldsymbol{\mu}+\boldsymbol{w}) \\ & && \text{(CC-SP3)} \\ \text{s.t. } & \boldsymbol{a}_i^{\mathrm{T}}\boldsymbol{x} + (\boldsymbol{y}_1^{\mathrm{T}}\boldsymbol{B}_i^{\mathrm{T}} + \boldsymbol{c}_i^{\mathrm{T}}\boldsymbol{H})\boldsymbol{\mu} + \boldsymbol{c}_i^{\mathrm{T}}\boldsymbol{w} + \\ & \Phi^{-1}(1-\gamma_i)\sqrt{(\boldsymbol{y}_1^{\mathrm{T}}\boldsymbol{B}_i^{\mathrm{T}} + \boldsymbol{c}_i^{\mathrm{T}}\boldsymbol{H})^{\mathrm{T}}\Sigma(\boldsymbol{y}_1^{\mathrm{T}}\boldsymbol{B}_i^{\mathrm{T}} + \boldsymbol{c}_i^{\mathrm{T}}\boldsymbol{H})} \\ & \leqslant g_i \ \forall i = 1,2,\ldots,M, \\ & \boldsymbol{A}'\boldsymbol{x} + \boldsymbol{C}'\boldsymbol{w} = \boldsymbol{0}, && (6) \\ & \boldsymbol{B}_k'\boldsymbol{y}_1 + (\boldsymbol{C}'\boldsymbol{H})_{:,k} = \boldsymbol{0}, && (7) \\ & -\boldsymbol{h}_j^{\mathrm{T}}\boldsymbol{\mu} - w_j + \Phi^{-1}(1-\lambda_j)\sqrt{\boldsymbol{h}_j^{\mathrm{T}}\Sigma\boldsymbol{h}_j} \leqslant 0, \\ & \forall j = 1,2,\ldots,N_2, \end{aligned}$$

$$\sum_{j=1}^{N_2} \lambda_j + \sum_{i=1}^{M} \gamma_i = \epsilon$$
$$\boldsymbol{x} \in \{0,1\} \cap \Pi,\ \boldsymbol{0} \leqslant \boldsymbol{y}_1,$$

where $\Phi^{-1}$ is the standard inverse cumulative distribution function (CDF) and $\Sigma = \text{diag}(\boldsymbol{\sigma}^2)$ is the covariance matrix. Eqs. (6) and (7) are derived from (4) such that the constant and stochastic terms are zero, respectively. $(\boldsymbol{C}'\boldsymbol{H})_{:,k}$ represents $k^{th}$ column of the matrix $\boldsymbol{C}'\boldsymbol{H}$. In next subsections, we will discuss how to solve (CC-SP3) to the global optimum.

### B. Outer Approximation

The function $\Phi^{-1}$ should be numerically approximated because it does not have an analytical form. Here we follow the outer approximation method developed by Cheng et al. [21]. A graphical demonstration of outer approximation is shown in Fig. 1 with $l^{th}$ cutting plane $v \geqslant t_l \epsilon + s_l$. The tangent $t_l$ and interception $v_l$ are:

$$t_l = \left.\frac{d\Phi^{-1}(1-\epsilon)}{d(\epsilon)}\right|_{\epsilon=\epsilon_l} = \frac{-1}{\phi(\Phi^{-1}(1-\epsilon_l))},$$
$$s_l = \Phi^{-1}(1-\epsilon_l) - t_l\epsilon_l,$$

where $\epsilon_l$ is the sampled point in the risk level space and $\phi$ is the standard probability distribution function of a normal distribution. In order to tightly approximate the function $\Phi^{-1}$, a large number of sampling points are recommended. In [24], an adaptive outer approximation scheme was developed to reduce the computational complexity while improving the approximation accuracy.

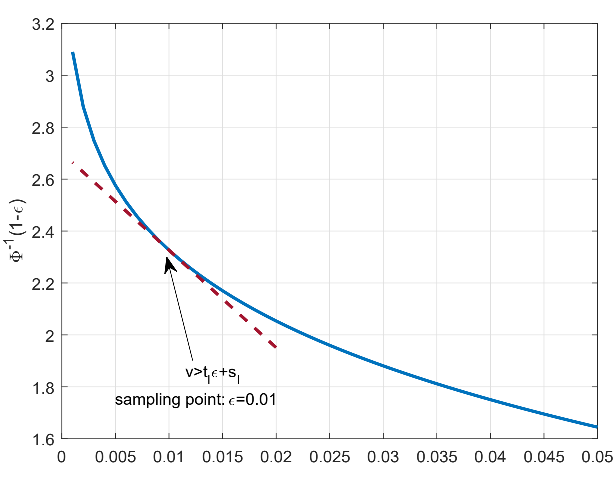


Fig. 1. The outer approximation of $\Phi^{-1}$.

### C. Branch-and-Bound

By replacing $\Phi^{-1}$ with $v$, (CC-SP3) becomes a mixed integer bi-convex problem:

$$\min_{\boldsymbol{x},\boldsymbol{y}_1,\boldsymbol{H},\boldsymbol{w},\boldsymbol{\gamma},\boldsymbol{\lambda}} \boldsymbol{q}^{\mathrm{T}}\boldsymbol{x} + \boldsymbol{p}_1^{\mathrm{T}}\boldsymbol{y}_1 + \boldsymbol{p}_2^{\mathrm{T}}(\boldsymbol{H}\boldsymbol{\mu} + \boldsymbol{w}) \qquad \text{(CC-SP4)}$$

$$\text{s.t. } \boldsymbol{a}_i^{\mathrm{T}}\boldsymbol{x} + (\boldsymbol{y}_1^{\mathrm{T}}\boldsymbol{B}_i^{\mathrm{T}} + \boldsymbol{c}_i^{\mathrm{T}}\boldsymbol{H})\boldsymbol{\mu} + \boldsymbol{c}_i^{\mathrm{T}}\boldsymbol{w} +$$
$$v_{\gamma_i}\sqrt{(\boldsymbol{y}_1^{\mathrm{T}}\boldsymbol{B}_i^{\mathrm{T}} + \boldsymbol{c}_i^{\mathrm{T}}\boldsymbol{H})^{\mathrm{T}}\Sigma(\boldsymbol{y}_1^{\mathrm{T}}\boldsymbol{B}_i^{\mathrm{T}} + \boldsymbol{c}_i^{\mathrm{T}}\boldsymbol{H})}$$
$$\leqslant g_i\ \forall i = 1,2,\ldots,M,$$
$$\boldsymbol{A}'\boldsymbol{x} + \boldsymbol{C}'\boldsymbol{w} = \boldsymbol{0},$$
$$\boldsymbol{B}_k'\boldsymbol{y}_1 + (\boldsymbol{C}'\boldsymbol{H})_{:,k} = \boldsymbol{0},$$
$$-\boldsymbol{h}_j^{\mathrm{T}}\boldsymbol{\mu} - w_j + v_{\lambda_j}\sqrt{\boldsymbol{h}_j^{\mathrm{T}}\Sigma\boldsymbol{h}_j} \leqslant 0, \forall j = 1,2,\ldots,N_2,$$
$$\sum_{j=1}^{N_2} \lambda_j + \sum_{i=1}^{M} \gamma_i = \epsilon,$$
$$v_{\lambda_j} \geqslant t_l(1-\lambda_j) + s_l,\ \forall l,\ \forall j,$$
$$v_{\gamma_i} \geqslant t_l(1-\gamma_i) + s_l,\ \forall l,\ \forall i,$$
$$\boldsymbol{x} \in \{0,1\} \cap \Pi,\ \boldsymbol{0} \leqslant \boldsymbol{y}_1.$$

Apart from integer variables, the non-convex terms lie in $v_{\lambda_j}\sqrt{\boldsymbol{h}_j^{\mathrm{T}}\Sigma\boldsymbol{h}_j}$ and $v_{\gamma_i}\sqrt{(\boldsymbol{y}_1^{\mathrm{T}}\boldsymbol{B}_i^{\mathrm{T}} + \boldsymbol{c}_i^{\mathrm{T}}\boldsymbol{H})^{\mathrm{T}}\Sigma(\boldsymbol{y}_1^{\mathrm{T}}\boldsymbol{B}_i^{\mathrm{T}} + \boldsymbol{c}_i^{\mathrm{T}}\boldsymbol{H})}$. Let us introduce auxiliary variables to represent the following bilinear terms, respectively.

$$z_{\lambda_j,m} = v_{\lambda_j}h_{j,m},\ z_{\gamma_i,m,n} = v_{\gamma_i}h_{m,n},\ d_{\gamma_i,m} = v_{\gamma_i}y_{1,m},$$

where $h_{m,n}$ represents the $m^{th}$ row, $j^{th}$ column element of $\boldsymbol{H}$. $y_{1,m}$ is $m^{th}$ element of $\boldsymbol{y}_1$. The bilinear terms can be convexified by the McCormick relaxation [22] when their upper and lower bounds are known:

$$z_{\lambda_j,m} \geqslant \underline{v}_{\lambda_j}h_{j,m} + v_{\lambda_j}\underline{h}_{j,m} - \underline{v}_{\lambda_j}\underline{h}_{j,m} \quad (8)$$
$$z_{\lambda_j,m} \geqslant \overline{v}_{\lambda_j}h_{j,m} + v_{\lambda_j}\overline{h}_{j,m} - \overline{v}_{\lambda_j}\overline{h}_{j,m} \quad (9)$$
$$z_{\lambda_j,m} \leqslant \underline{v}_{\lambda_j}h_{j,m} + v_{\lambda_j}\overline{h}_{j,m} - \underline{v}_{\lambda_j}\overline{h}_{j,m} \quad (10)$$
$$z_{\lambda_j,m} \leqslant \overline{v}_{\lambda_j}h_{j,m} + v_{\lambda_j}\underline{h}_{j,m} - \overline{v}_{\lambda_j}\underline{h}_{j,m} \quad (11)$$
$$z_{\gamma_i,m,n} \geqslant \underline{v}_{\gamma_i}h_{m,n} + v_{\gamma_i}\underline{h}_{m,n} - \underline{v}_{\gamma_i}\underline{h}_{m,n} \quad (12)$$
$$z_{\gamma_i,m,n} \geqslant \overline{v}_{\gamma_i}h_{m,n} + v_{\gamma_i}\overline{h}_{m,n} - \overline{v}_{\gamma_i}\overline{h}_{m,n} \quad (13)$$
$$z_{\gamma_i,m,n} \leqslant \underline{v}_{\gamma_i}h_{m,n} + v_{\gamma_i}\overline{h}_{m,n} - \underline{v}_{\gamma_i}\overline{h}_{m,n} \quad (14)$$
$$z_{\gamma_i,m,n} \leqslant \overline{v}_{\gamma_i}h_{m,n} + v_{\gamma_i}\underline{h}_{m,n} - \overline{v}_{\gamma_i}\underline{h}_{m,n} \quad (15)$$
$$d_{\gamma_i,m} \geqslant \underline{v}_{\gamma_i}y_{1,m} + v_{\gamma_i}\underline{y}_{1,m} - \underline{v}_{\gamma_i}\underline{y}_{1,m} \quad (16)$$
$$d_{\gamma_i,m} \geqslant \overline{v}_{\gamma_i}y_{1,m} + v_{\gamma_i}\overline{y}_{1,m} - \overline{v}_{\gamma_i}\overline{y}_{1,m} \quad (17)$$
$$d_{\gamma_i,m} \leqslant \underline{v}_{\gamma_i}y_{1,m} + v_{\gamma_i}\overline{y}_{1,m} - \underline{v}_{\gamma_i}\overline{y}_{1,m} \quad (18)$$
$$d_{\gamma_i,m} \leqslant \overline{v}_{\gamma_i}y_{1,m} + v_{\gamma_i}\underline{y}_{1,m} - \overline{v}_{\gamma_i}\underline{y}_{1,m} \quad (19)$$

Given these relaxations, a lower bounding problem can be established:

$$\min_{\boldsymbol{x},\boldsymbol{y}_1,\boldsymbol{H},\boldsymbol{w},\boldsymbol{\gamma},\boldsymbol{\lambda}} \boldsymbol{q}^{\mathrm{T}}\boldsymbol{x} + \boldsymbol{p}_1^{\mathrm{T}}\boldsymbol{y}_1 + \boldsymbol{p}_2^{\mathrm{T}}(\boldsymbol{H}\boldsymbol{\mu} + \boldsymbol{w}) \qquad \text{(LBP)}$$

$$\text{s.t. } \boldsymbol{a}_i^{\mathrm{T}}\boldsymbol{x} + (\boldsymbol{y}_1^{\mathrm{T}}\boldsymbol{B}_i^{\mathrm{T}} + \boldsymbol{c}_i^{\mathrm{T}}\boldsymbol{H})\boldsymbol{\mu} + \boldsymbol{c}_i^{\mathrm{T}}\boldsymbol{w} +$$
$$\sqrt{(\boldsymbol{d}_{\gamma_i}^{\mathrm{T}}\boldsymbol{B}_i^{\mathrm{T}} + \boldsymbol{c}_i^{\mathrm{T}}\boldsymbol{Z}_{\gamma_i})^{\mathrm{T}}\Sigma(\boldsymbol{d}_{\gamma_i}^{\mathrm{T}}\boldsymbol{B}_i^{\mathrm{T}} + \boldsymbol{c}_i^{\mathrm{T}}\boldsymbol{Z}_{\gamma_i})}$$
$$\leqslant g_i\ \forall i = 1,2,\ldots,M,$$
$$\boldsymbol{A}'\boldsymbol{x} + \boldsymbol{C}'\boldsymbol{w} = \boldsymbol{0},$$
$$\boldsymbol{B}_k'\boldsymbol{y}_1 + (\boldsymbol{C}'\boldsymbol{H})_{:,k} = \boldsymbol{0},$$
$$-\boldsymbol{h}_j^{\mathrm{T}}\boldsymbol{\mu} - w_j + \sqrt{\boldsymbol{z}_{\lambda_j}^{\mathrm{T}}\Sigma\boldsymbol{z}_{\lambda_j}} \leqslant 0, \forall j = 1,2,\ldots,N_2,$$

$$\sum_{j=1}^{N_2}\lambda_j+\sum_{i=1}^{M}\gamma_i=\epsilon,$$
$$v_{\lambda_j}\geqslant t_l(1-\lambda_j)+s_l,\ \forall l,\ \forall j,$$
$$v_{\gamma_i}\geqslant t_l(1-\gamma_i)+s_l,\ \forall l,\ \forall i,$$
$$\text{Eq. }(8)-(19),$$
$$\boldsymbol{x}\in\{0,1\}\cap\Pi,\ \mathbf{0}\leqslant\boldsymbol{y}_1.$$

(LBP) is a mixed-integer second-order cone program (MI-SOCP) that can be solved by CPLEX to generate possible risk level solution $\gamma_i^*$ and $\lambda_j^*$ if it is feasible. Substituting such risk level solutions into (CC-SP3), the resulting problem is still an MI-SOCP, serving as the upper bound (UB) solution. The relaxation gap of (LBP) is dependent on the distance between lower and upper bounds. As the variable range becomes smaller, the relaxation gap can be tightened. To this end, we continuously branch the variable in $\boldsymbol{h}$ or $\boldsymbol{y}_1$ to lift the solution of (LBP). A conventional way to choose the branching variable at each iteration is comparing the products and auxiliary variable in the solution of (LBP):

$$\{i',j',m',n'\}=\arg\max\big\{|z^*_{\lambda_j,m}-v^*_{\lambda_j}h^*_{j,m}|,\\ |z^*_{\gamma_i,m,n}-v^*_{\gamma_i}h^*_{m,n}|,\ |d^*_{\gamma_i,m}-v^*_{\gamma_i}y^*_{1,m}|\big\}$$

Then, we branch the chosen variable at the current (LBP) solution value and create two nodes, representing new (LBP), on the searching-tree. If the solution of that (LBP) is greater than the existing UB, then such a node can be discarded without branching. The lower bound solution (LB) is defined as the lowest value of the (LBP) solution on the searching-tree. When LB is equal to UB, a global optimum solution is found. Here we need to remark that finding a true global optimum solution, namely, UB = LB can be time-consuming. To this end, the relative gap, defined as $\frac{UB-LB}{|LB|}$, is specified to terminate the global optimization and forward such an optimal solution for posterior evaluation. Alternatively, the global optimization can be terminated if all nodes in the searching tree have been enumerated.

### D. Bound Tightening

Branch-and-bound can only reduce the range of one variable at each time whereas the proposed optimization-based bound tightening (OBBT) scheme updates $\boldsymbol{H}$ and $\boldsymbol{y}_1$ bounds at each iteration. The (OBBT) needs to solve the following MI-SOCP optimizations for each variable in vector $\boldsymbol{y}_1$ and $\boldsymbol{H}$:

$$\max\ \text{or}\ \min\ y_{1,m}\ \text{or}\ h_{m,n} \tag{OBBT}$$
$$\text{s.t.}\ \boldsymbol{a}_i^{\mathrm{T}}\boldsymbol{x}+(\boldsymbol{y}_1^{\mathrm{T}}\boldsymbol{B}_i^{\mathrm{T}}+\boldsymbol{c}_i^{\mathrm{T}}\boldsymbol{H})\boldsymbol{\mu}+\boldsymbol{c}_i^{\mathrm{T}}\boldsymbol{w}+$$
$$\sqrt{(\boldsymbol{d}_{\gamma_i}^{\mathrm{T}}\boldsymbol{B}_i^{\mathrm{T}}+\boldsymbol{c}_i^{\mathrm{T}}\boldsymbol{Z}_{\gamma_i})^{\mathrm{T}}\Sigma(\boldsymbol{d}_{\gamma_i}^{\mathrm{T}}\boldsymbol{B}_i^{\mathrm{T}}+\boldsymbol{c}_i^{\mathrm{T}}\boldsymbol{Z}_{\gamma_i})}$$
$$\leqslant g_i\ \forall i=1,2,\ldots,M,$$
$$\boldsymbol{A}'\boldsymbol{x}+\boldsymbol{C}'\boldsymbol{w}=\mathbf{0},$$
$$\boldsymbol{B}'_k\boldsymbol{y}_1+(\boldsymbol{C}'\boldsymbol{H})_{:,k}=\mathbf{0},$$
$$-\boldsymbol{h}_j^{\mathrm{T}}\boldsymbol{\mu}-w_j+\sqrt{\boldsymbol{z}_{\lambda_j}^{\mathrm{T}}\Sigma\boldsymbol{z}_{\lambda_j}}\leqslant 0,\forall j=1,2,\ldots,N_2,$$
$$\sum_{j=1}^{N_2}\lambda_j+\sum_{i=1}^{M}\gamma_i=\epsilon,$$
$$v_{\lambda_j}\geqslant t_l(1-\lambda_j)+s_l,\ \forall l,\ \forall j,$$
$$v_{\gamma_i}\geqslant t_l(1-\gamma_i)+s_l,\ \forall l,\ \forall i,$$
$$\text{Eq. }(8)-(19),$$
$$\boldsymbol{q}^{\mathrm{T}}\boldsymbol{x}+\boldsymbol{p}_1^{\mathrm{T}}\boldsymbol{y}_1+\boldsymbol{p}_2^{\mathrm{T}}(\boldsymbol{H}\boldsymbol{\mu}+\boldsymbol{w})\leqslant\text{UB}, \tag{20}$$
$$\boldsymbol{x}\in\{0,1\}\cap\Pi,\ \mathbf{0}\leqslant\boldsymbol{y}_1.$$

(OBBT) inherits the formula of (LBP) but changes the objective function. In addition, (OBBT) introduces constraint (20) to eliminate the variable range resulting to non-optimal (greater than the existing UB) solution value. The bound tightening is critical to the optimization of (CC-SP3) because the range of $\boldsymbol{H}$ is unknown in prior. A wide interval of variables in $\boldsymbol{H}$ is assumed initially, which should be further reduced through the bound tightening. There are $2(N_2\times K+N_1)$ MI-SOCP to solve at each iteration for bound tightening. If the dimensions of $\boldsymbol{H}$ and $\boldsymbol{y}_1$ are high, we may relax the integer constraint to solve a SOCP instead of MI-SOCP for each variable to yield loose but valid bounds.

### E. Posterior Evaluation and Balas Cut

The linear decision-rule offers a conservative solution for stage-II variables. However, once the stage-I decision is made and the uncertainty is revealed, the actual performance in stage-II can be improved through optimization rather than relying solely on the decision-rule. To this end, we propose the scenario-based posterior evaluation to further quantify the quality of each stage-I solution. Namely, when a satisfactory solution of (CC-SP3) is achieved, the stage-I variables are fixed and the stage-II variables are optimized according to the parameters of each sampled scenario. The expected objective function value can be approximated by the mean of all sampled objective function value. The probabilistic feasibility is verified by counting the number of infeasible scenarios. In order to find a satisfactory solution, this solving procedure should be repeated. Because stage-I variables should be integers, the Balas cut can be employed to exclude the stage-I solution previously visited. The form of Balas cut is shown in Eq (21).

$$\sum_{j\in\{r:x_r^*=1\}}x_j-\sum_{i\in\{r:x_r^*=0\}}x_i\leqslant|\{r:x_r^*=1\}|-1, \tag{21}$$

where $|\cdot|$ is the cardinality of a set and $x^*$ represents the stage-I solution of (LBP). By integrating the Balas cut into (LBP) and (OBBT), any (LBP) solutions obtained in the previous iterations will not be revisited again. We can thus search for the first, second, and more optima to form a solution pool. The posterior evaluation will show the true performance of the stage-I solution pool. The overall solving procedure of CC-SP is shown in Fig. 2. Here we can pre-specify the required number of solutions in the pool to determine when the posterior evaluation algorithm can be terminated.

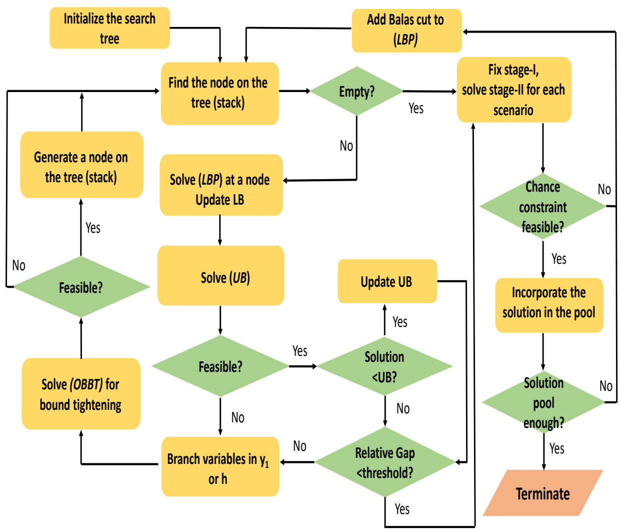


Fig. 2. The Algorithm Scheme.

## IV. Case Studies

A petroleum refinery with flowchart shown in Fig. 3 is optimized under the allowable risk level $\epsilon = 3\%$. We want to determine the amount of crude oil procurement at stage-I while operational conditions are subject to uncertainty. When crude oil is processed at stage-II, the flows of each unit can be adjusted to adapt uncertainties. The resulting two-stage SP is solved through GAMS 32.2.0 with an optimization solver CPLEX. The hardware platform is a laptop with i7-7500U CPU 2.70 GHZ with 8 GB memory.

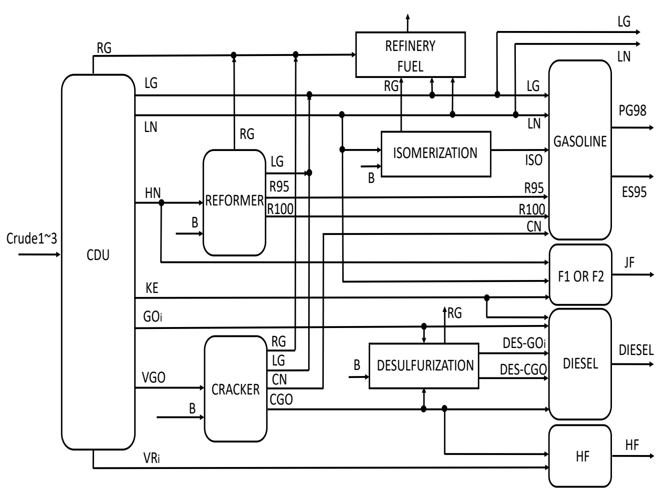


Fig. 3. The Refinery Flowchart.

### A. Stage-I

At stage-I, three types of crude oil are purchased with maximum capacity 1800000 bbl for each crude. The minimal procurement is 50000 bbl if such crude is selected. The crude oil yield is shown in Table I. The following constraints for

TABLE I
Crude Oil Yield (%)

| | RG | LG | LN | HN | KE | GO | VGO | VR |
|---|---|---|---|---|---|---|---|---|
| C1 | 0.2 | 0.91 | 6.98 | 15.98 | 10.03 | 28.76 | 26.82 | 10.32 |
| C2 | 0.2 | 0.80 | 6.10 | 12.06 | 8.61 | 24.14 | 26.46 | 21.63 |
| C3 | 0.4 | 2 | 8.51 | 15.32 | 9.47 | 25.39 | 25.35 | 13.56 |

stage-I variables are introduced [23]:

$$\sum_{j=1}^{9} 2^{j-1} x_{\text{Crude}_i,j} 5000 \geqslant 50000 x_{\text{purchase}_i},$$

$$x_{\text{Crude}_i,j} \leqslant x_{\text{purchase}_i}, \ \forall i \in \{1,2,3\}, \ \forall j \in \{1,2\ldots,9\},$$

where $x_{\text{Crude}_i,j} \in \{0,1\}$ is a binary variable to count purchase quantity. $x_{\text{purchase}_i} = 1$ implies choosing Crude$_i$ and $x_{\text{purchase}_i} = 0$ means no purchase of that crude. We assume that one lot may incorporate 5000 bbl. The decision maker needs to decide how many lots have to be purchased such that the profit is maximized and all quality specifications are met. Here we use 9 binary variables to represent the decimal number and thus the Balas cut can be adopted to eliminate previously visited stage-I solutions. Liquefied gas (LG), liquefied naphtha (LN), Gasoline98, Gasoline95, kerosene (KE), jet fuel, diesel and heavy fuel oil (HF) are products to be sold in the market. The cost includes desulfurization and crude oil procurement. Therefore, the objective function for optimization including stage-I and II is shown in Eq. (22):

$$\begin{aligned}\text{Profit} = {} & \text{Revenue of LG, LN, Gasoline98, Gasoline95,} \\ & \text{KE, Jet Fuel, Diesel, and HF} - \text{Desulfurization cost} \\ & - \text{Crude oil procurement cost} \qquad (22)\end{aligned}$$

### B. State-II

At stage-II, the inflows and outflows of each unit are determined after the uncertainty realization. The quality specification of each product, demands, and the capacity of each unit are shown in Table II. The mass balance and quality inequalities can be found from [16]. However, three uncertain parameters are newly introduced into the stage-II model, including $\theta_S \sim \mathcal{N}(0, 0.004^2)$: the remained sulfur content after defurization; $\theta_{\text{Cracker-AGO}} \sim \mathcal{N}(0, 0.04^2)$ and $\theta_{\text{Cracker-Mogas}} \sim \mathcal{N}(0, 0.04^2)$ : change of cracker yield in AGO and Mogas modes, respectively. The equations directly involving these uncertainty parameters are listed below.

**Sulfur in Diesel:**

$$\begin{aligned}&\sum_i y_{\text{DIESEL,GO}_i} S_{\text{GO}_i} + \sum_i y_{\text{DESGO}_i} S_{\text{GO}_i} (2\% + \theta_S) + \\ & y_{\text{DIESEL,KE}} S_{\text{KE}} + y_{\text{DIESEL,DESCGO}} S_{\text{CGO}} (2\% + \theta_S) \\ & + y_{\text{DIESEL,CGO}} S_{\text{CGO}} \leqslant 50\text{ppm} \Big( y_{\text{DIESEL,KE}} + y_{\text{DIESEL,DESCGO}} \\ & + \sum_i (y_{\text{DIESEL,GO}_i} + y_{\text{DIESEL,DESGO}_i}) + y_{\text{DIESEL,CGO}} \Big).\end{aligned}$$

where $S$ denotes the sulfur content in the flow. Here we assume that the desulphurization unit may remove 98% of sulfur on average. However, the catalyst uncertainty $\theta_S$ may degrade the desulphurization unit performance and result in the sulfur constraint violation.

**Cat Cracked Gasoline (CN):**

$$\begin{aligned} & y_{\text{Cracker-Mogas,VGO}}(\text{P}_{\text{Cracker-Mogas,CN}} + \theta_{\text{Cracker-Mogas}}) \\ & + y_{\text{Cracker-AGO,VGO}}(\text{P}_{\text{Cracker-AGO,CN}} + \theta_{\text{Cracker-AGO}}) \\ & = y_{98,\text{CN}} + y_{95,\text{CN}}, \end{aligned} \tag{23}$$

**Light Cycle Oil (CGO):**

$$\begin{aligned} & y_{\text{Cracker-Mogas,VGO}}(\text{P}_{\text{Cracker-Mogas,CGO}} - \theta_{\text{Cracker-Mogas}}) \\ & + y_{\text{Cracker-AGO,VGO}}(\text{P}_{\text{Cracker-AGO,CGO}} - \theta_{\text{Cracker-AGO}}) \\ = & y_{\text{DIESEL,CGO}} + y_{\text{Des,CGO}} + y_{\text{HF,CGO}}, \end{aligned} \tag{24}$$

where P is the portion of each yield. The cracker may work on the Mogas and AGO modes with different yields. The CN and CGO yields may fluctuate under these modes. Because $\theta_{\text{Cracker-Mogas}}$ and $\theta_{\text{Cracker-AGO}}$ directly affect the flow of CN and CGO based on Eqs. (23) and (24), they indirectly impact the qualities of Gasoline98, Gasoline95, and diesel such that their specification may not fully met if only nominal parameters are considered in the optimization. All chance constraints are listed in Table II. Here max means the upper bound and min means lower bound on that quality.

TABLE II

QUALITY, DEMAND, AND CAPACITY

| Constraints | Bound | Risk level (%) |
|---|---|---|
| Gasoline98 RON (min) | 98 | 0.010 |
| Gasoline95 RON (min) | 95 | 0.010 |
| Gasoline98 Sulfur (max, ppm) | 15 | 0.0125 |
| Gasoline95 Sulfur (max, ppm) | 30 | 0.010 |
| Diesel Sulfur (max, ppm) | 50 | 2.170 |
| HFO Viscosity (max) | 30 | 0.638 |
| Gasoline98 (demand) | 15 | 0.010 |
| Diesel (demand) | 100 | 0.010 |
| Cracker (capacity) | 135 | 0.010 |
| Desulphur (capacity) | 130 | 0.010 |
| Reformer (capacity) | 65 | 0.010 |
| Distillation (capacity) | 700 | N/A |

To reduce the computational burden, we require the unit capacity and non-negative variable constraints to be satisfied with 99.99%. The distillation unit operation is determined at stage-I and thereby not affected by uncertainties. The remained risk budget should be distributed to totally 8 quality and demand constraints. In addition, the lowest violation ratio of each chance constraint is set as 0.01%. By using the proposed algorithm and setting the relative gap to be 0.1%, we explore top 8 solutions of (CC-SP4) and use 500 scenarios to evaluate their actual performance at stage-II. The risk level of each chance constraint is shown in the last column of Table II. The diesel sulfur is assigned with the largest risk level (2.17%) among all constraints due to the desulfurization uncertainty. The resulting scenario-based posterior evaluation profit, decision-rule derived profit, and crude procurement are shown in Table III. We can see that all these solutions have similar profit, which shows the challenge to find the global optimum. Due to the non-zero relative gap, we find the best solution at $3^{rd}$ iteration. The joint constraints violation ratio in the posterior evaluation is 1.2%, much lower than the desired 3%. The profit obtained through the decision-rule is slightly lower than that of posterior evaluation for each scenario, which implying the conservativeness of linear decision-rule. However, the proposed method spends only 673 seconds to obtain all these 8 solutions and avoids solving the large-scale MILP formula introduced by the scenario tree.

TABLE III

OPTIMIZATION RESULTS

| Three crude oil procurement (ton) | Posterior evaluation profit ($10^3$\$) | Decision-rule profit ($10^3$\$) |
|---|---|---|
| 48.311, 241.555, 218.871 | 110755.7 | 110035.3 |
| 48.311, 240.884, 219.537 | 110752.5 | 110032.7 |
| 47.640, 241.555, 219.537 | **110761.4** | **110038.1** |
| 48.982, 241.555, 218.206 | 110750.0 | 110032.4 |
| 48.982, 240.884, 218.871 | 110746.9 | 110029.8 |
| 49.653, 241.555, 217.541 | 110744.3 | 110029.0 |
| 49.653, 240.884, 218.206 | 110741.2 | 110026.5 |
| 50.324, 241.555, 216.876 | 110738.6 | 110026.2 |

## V. CONCLUSION

This paper presents a methodology to solve the two-stage chance-constrained SP in complex system optimization. The linear decision-rule is employed to parameterize the stage-II variable as a function of normally-distributed uncertainty. The resulting formulation can be transferred into a lower bounding problem using outer approximation and McCormick relaxation techniques. Additionally, an upper bound problem can be established by fixing the risk level of joint chance constraints. By iteratively solving the lower and upper bounding problems, a global optimum of linear decision-rule can be obtained. Furthermore, scenario-based posterior evaluation and Balas cut are applied to quantify and improve the stage-II decisions. The crude oil procurement and plant operations for a simplified refinery model is optimized to show the effectiveness of proposed algorithms. In the future work, more flexible decision-rule can be integrated into this framework to improve the optimality of the solution.

## REFERENCES


[1] M. G. Ierapetritou, E. N. Pistikopoulos, C. A. Floudas, "Operational planning under uncertainty," *Computers & Chemical Engineering*, vol. 20, pp. 1499-1516, 1996.

[2] V. Bansal, J. D. Perkins, E. N. Pistikopoulos, "Flexibility analysis and design of dynamic processes with stochastic parameters," *Computers & Chemical Engineering*, vol. 22, pp. 817-820, 1998.

[3] W. C.Rooney, L. T. Biegler, "Design for model parameter uncertainty using nonlinear confidence regions," *AIChE Journal*, vol. 47, pp. 1794-1804, 2001.

[4] K. Al-Qahtani, A. Elkamel, "Robust planning of multisite refinery networks: Optimization under uncertainty," *Computers & Chemical Engineering*, vol. 34, pp. 985-995, 2011.

[5] C. Ning, F. You, "Data-driven stochastic robust optimization: General computational framework and algorithm leveraging machine learning for optimization under uncertainty in the big data era," *Computers & Chemical Engineering*, vol. 111, pp. 115-133, 2018.

[6] D. Gupta, C. T. Maravelias, "Framework for studying online production scheduling under endogenous uncertainty," *Computers & Chemical Engineering*, vol. 135, pp. 106670, 2020.

[7] N. V. Sahinidis, “Optimization under uncertainty: state-of-the-art and opportunities,” *Computers & Chemical Engineering*, vol. 28, pp. 971-983, 2004.

[8] I. E. Grossmann, R. M. Apap, B. A. Calfa, P. García-Herreros, Q. Zhang. “Recent advances in mathematical programming techniques for the optimization of process systems under uncertainty,” *Computers & Chemical Engineering*, vol. 91, pp. 3-14, 2016.

[9] J. F. Benders, “Partitioning procedures for solving mixed-variables programming problems,” *Numerische Mathematik*, vol. 4, pp. 238-252, 1962.

[10] A. M. Geoffrion, “Generalized Benders decomposition,” *Journal of Optimization Theory and Applications*, vol. 10, pp. 237-260, 1972.

[11] R. Karuppiah, I. E. Grossmann, “A Lagrangean based branch-and-cut algorithm for global optimization of nonconvex mixed-integer nonlinear programs with decomposable structures,” *Journal of Global Optimization*, vol. 41, pp. 163-186, 2008.

[12] S. Mouret, I. E. Grossmann, P. Pestiaux, “A new Lagrangian decomposition approach applied to the integration of refinery planning and crude-oil scheduling,” *Computers & Chemical Engineering*, vol. 35, pp. 2750-2766, 2011.

[13] N. K. Shah, M. G. Ierapetritou, “Lagrangian decomposition approach to scheduling large-scale refinery operations,” *Computers & Chemical Engineering*, vol. 79, pp. 1-29, 2015.

[14] X. Liu, S. Küçükyavuz, J. Luedtke, “Decomposition algorithms for two-stage chance-constrained programs,” *Mathematical Programming*, vol. 157, pp. 219-243, 2016.

[15] J. Luedtke, “A branch-and-cut decomposition algorithm for solving chance-constrained mathematical programs with finite support,” *Mathematical Programming*, vol. 146, pp. 219-244, 2014.

[16] Y. Yang, “Improved benders decomposition and feasibility validation for two-stage chance-constrained programs in process optimization,” *Industrial & Engineering Chemistry Research*, vol. 58, pp. 4853-4865, 2019.

[17] X. Chen, M. Sim, P. Sun, J. W. Zhang, “A linear decision-based approximation approach to stochastic programming,” *Operations Research*, vol. 56, pp. 344-357, 2008.

[18] S. Rahal, Z. Li, D. J. Papageorgiou, “Deep lifted decision rules for two-stage adaptive optimization problems,” *Computers & Chemical Engineering*, vol. 159, pp. 107661, 2022.

[19] E. Balas, R. Jeroslow, “Canonical cuts on the unit hypercube,” *SIAM Journal of Applied Mathematics*, vol. 23, pp. 61-69, 1972.

[20] A. Prékoba, *Stochastic programming*; Netherlands: Kluwer Academic Publishers, 1995.

[21] J. Cheng, C. Gicquel, A. Lisser, “A second-order cone programming approximation to joint chance-constrained linear programs,” *Lecture Notes in Computer Science*, vol. 7422, pp. 71-80, 2012.

[22] G. P. McCormick, “Computation of global solutions to factorable nonconvex programs: Part I convex underestimating problems,” *Mathematical Programming*, vol. 10, pp. 147-175, 1976.

[23] Y. Yang, P. I. Barton, “Integrated crude selection and refinery optimization under uncertainty,” *AIChE Journal*, vol. 62, pp. 1038-1053, 2016.

[24] Y. Yang, V. Phebe, P. Barton, “Chance-constrained optimization for refinery blend planning under uncertainty,” *Industrial & Engineering Chemistry Research*, vol. 56, pp. 12139-12150, 2017.